

Entrainment in a stochastic computational model of basal ganglia dynamics in Parkinson's Disease

Joseph Wimmergren and Brandon Zhu

Section 1 - Background and Motivation

Motivation:

Parkinson's disease (PD) is the second most common neurodegenerative disorder (only behind Alzheimer's). Some common symptoms of PD are tremor, bradykinesia, stiffness, sleep disturbance, depression, and anxiety.

PD is characterized by the loss of dopaminergic neurons in the basal ganglia (BG). The primary function of the BG is likely to control and regulate the dynamics of the motor and premotor cortical areas so that voluntary movements can be performed smoothly and involuntary movements are inhibited. The complex network-level dynamics in the basal ganglia eventually lead to the GPi sending inhibitory signals to the thalamus. The thalamus (TH), in a healthy individual, is responsible for faithfully relaying information from the sensorimotor cortex (SMC). The development of Parkinson's disease is associated with changes in BG neuronal firing rates. In particular, bursting and oscillatory behavior are key electrophysiological behaviors evident in the parkinsonian brain. The oscillatory and bursting inhibitory signal sent from the GPi to the TH prevents the TH from relaying the SMC signals faithfully, and the characteristic PD motor abnormalities arise [1].

Pharmaceutical therapeutic options are limited, but levodopa (L-DOPA) and carbidopa (in tandem) are widely used. L-DOPA is broken down into dopamine in the brain, and carbidopa prevents the levodopa from being broken down before it gets to the brain. However, prescribing levodopa and carbidopa dosage is a messy process. It may take a Parkinson's patient years before their levodopa/carbidopa "cocktail" dosage is right for them [2]. The side effects of L-DOPA are also points of concern for many patients. L-DOPA is effective for only 4-10 years, and the daily quality of life fluctuates greatly for PD patients because of the inherent pharmacokinetics of the body that result in characteristic "on and off times" of the drug. After taking L-DOPA, the patient will experience a moment where the concentration of L-DOPA in their body is optimized for their PD and their pathological symptoms are momentarily diminished -- this is called the "on time". As they are coming down from L-DOPA and until they can take L-DOPA again, many PD patients often experience more severe PD symptoms than they would without even taking L-DOPA in the first place [2]. Long term use of L-DOPA also results in a permanent side effect called dyskinésias. Dyskinésias are involuntary, writhing movements of the body. As such, PD patients are forced to make an uncomfortable decision about whether they want to have 4-10

“good” years of on and off time, followed by the rest of their life of dyskinesias, or just take the full wrath of Parkinson’s disease head-on [2].

There are surgical methods of alleviating PD symptoms. A complicated and somewhat dark history of brain surgeries led to the two most common surgical procedures: lesioning and deep brain stimulation. In the lesioning treatment, the surgeon makes small slices or ablations in the patient’s STN or GPi, causing scar tissue. This is thought to eliminate the pathological output from the BG to the TH. However, this surgery has a high risk of causing permanent hemiballism, the violent, involuntary, high amplitude movement of the patient’s limbs. As such, this surgery has been phasing out of the mainstream therapeutics for PD and is being replaced by deep brain stimulation. Lesion surgeries are still done today, but only as a last resort [2].

Deep brain stimulation (DBS) is an FDA approved (often reversible) surgery wherein a lead is placed in the patient’s brain (usually STN or GPi) and stimulated with high frequency (120-150 Hz) pulses (e.g. 300 μ A/cm²) [1] [2]. This surgery is not an exact science yet. Stimulation parameters are often found through trial and error, and the lead placement varies not only between patients, but also between physicians. Although the clinical efficacy of DBS in alleviating PD symptoms is well established, the mechanism of action is unknown.

Stimulation-induced modulation of the pathological network activities represents the most likely mechanism of action for DBS. STN-DBS leads to tonic, high frequency spiking in the STN, which has an excitatory effect on the GPi [1]. As such, the GPi cells fire tonically, and regular inhibitory signals are sent to the thalamus, which restore the thalamic relay capability seen in a healthy patient [1]. Therefore, modeling the dynamics of the basal ganglia-thalamic network with deep brain stimulation is of particular interest.

In a variety of different neural systems, it has been found that the activation of single neurons is strongly influenced by the characteristics of the stimulus pattern. For example, Mainen and Sejnowski showed that in neocortical neurons, suprathreshold DC stimulus evoked randomly fluctuating neural responses that had low repeatability over multiple trials [3]. Although the overall firing frequency remained consistent, the exact timing of the firing varied drastically. In contrast, noisy signals (Gaussian white noise) were able to evoke reliable responses that became entrained (synchronized) to the stimulus [3] [4]. These results indicate that noisy input plays an important role in neuron spiking patterns, and the noise of a neural signal may encode important neural information [3] [4]. While this paper applies this concept primarily to synaptic inputs, it can be inferred that this may also apply to extracellular stimulation. As such, it is interesting to consider whether constant stimuli, which are customary in DBS, are evoking similar fluctuations. It may be possible that a noisy input may lead to more consistent response patterns that could increase the therapeutic efficacy of DBS. By investigating various deep brain stimulation regimes in a basal ganglia - thalamic network model, it may be possible to further develop an

understanding of the mechanisms underlying DBS and improve its therapeutic efficacy for PD patients.

Section 2 - Model and Methods

Basal Ganglia - Thalamic Network Model

A single compartment basal ganglia-thalamic network model in MATLAB from [1] formed the framework for our novel additions. This model is comprised of thalamic (TH), subthalamic nucleus (STN), and globus pallidus pars externa and interna (GPe and GPi) neurons, interconnected to form a 10 cell per population network which responds to stimulus from the sensorimotor cortex (SMC).

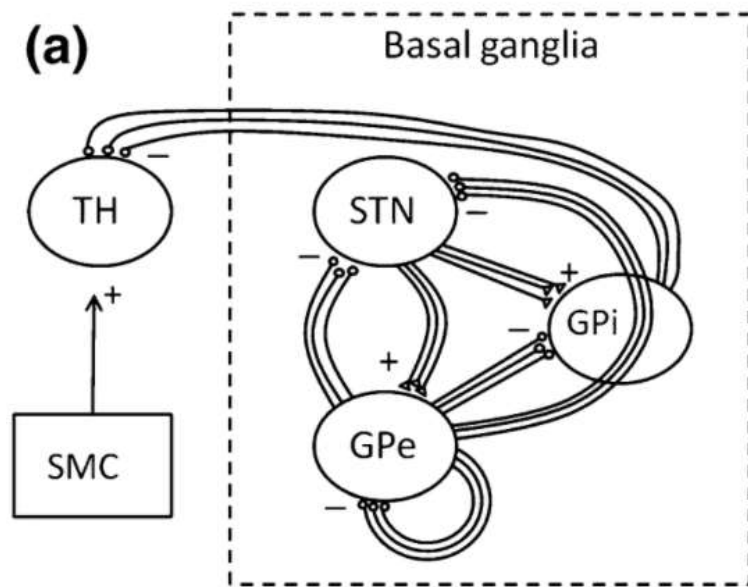


Figure 1: Schematic from [1] for the basal ganglia-thalamic network. Circles represent inhibitory connections, and triangles represent excitatory connections.

These populations of cells were connected in a sparse but structured way. Each STN cell projects to two neighboring GPe and GPi cells. Each GPe cell projects to two neighboring STN, GPe, and GPi cells, and each GPi cell projects to one TH cell. The membrane potentials from the different regions simulated were governed by the H-H type equations and parameters below.

Thalamus

$$C_m v' = -I_L - I_{Na} - I_K - I_T - I_{GPI \rightarrow Th} + I_{SMC}$$

$$h' = [h_\infty(v) - h]/\tau_h(v)$$

$$r' = [r_\infty(v) - r]/\tau_r(v)$$

[1]

Where I_L is the leak current, I_{Na} is the sodium current, I_K is the potassium current, I_T is the low threshold potassium current, $I_{GPI \rightarrow Th}$ is the synaptic current from the GPI to the TH, and I_{SMC} is the current pulse from the sensorimotor cortex. The corresponding equations, gating variables, and parameters for the thalamus are listed in table 1.

Table 1 TH cell model equations and parameters

Current	Equation	Gating variables	Gating variables	Parameters
I_L	$g_L(v - E_L)$			$g_L = 0.05$ $E_L = -70$
I_{Na}	$g_{Na} m_\infty(v)^3 h(v - E_{Na})$	$m_\infty(v) = 1/[1 + \exp(-\frac{v+37}{7})]$	$h_\infty(v) = 1/[1 + \exp(\frac{v+41}{4})]$ $\tau_h(v) = 1/[0.128 \exp(-\frac{v+46}{18}) + 4/(1 + \exp(-\frac{v+23}{5}))]$	$g_{Na} = 3$ $E_{Na} = 50$
I_K	$g_K[0.75(1 - h)](v - E_K)$	*same h as in I_{Na}		$g_K = 5$ $E_K = -75$
I_T	$g_T p_\infty(v)^2 r(v - E_T)$	$p_\infty(v) = 1/[1 + \exp(-\frac{v+60}{6.2})]$	$r_\infty(v) = 1/[1 + \exp(\frac{v+84}{4})]$ $\tau_r(v) = 0.15[28 + \exp(-\frac{v+25}{10.5})]$	$g_T = 5$ $E_T = 0$

[1]

Subthalamic Nucleus

$$C_m v' = -I_L - I_{Na} - I_K - I_T - I_{Ca} - I_{ahp} - I_{GPe \rightarrow STN} + I_{app} + I_{dbs}$$

$$h' = 0.75[h_\infty(v) - h]/\tau_h(v)$$

$$n' = 0.75[n_\infty(v) - n]/\tau_n(v)$$

$$r' = 0.2[r_\infty(v) - r]/\tau_r(v)$$

$$c' = 0.08[c_\infty(v) - c]/\tau_c(v)$$

$$CA' = 3.75 \times 10^{-5}(-I_{Ca} - I_T - 22.5 \times CA)$$

[1]

Where I_{Ca} is the calcium current, I_{ahp} is the afterhyperpolarization current, $I_{GPe \rightarrow STN}$ is the synaptic current from the GPe to the STN, I_{app} is the bias current modeled as the net synaptic input to cells from other brain regions, and I_{dbs} is the deep brain stimulation current.

Table 2 STN cell model equations and parameters

Current	Equation	Gating variables	Gating variables	Parameters
I_L	$g_L(v - E_L)$			$g_L = 2.25$ $E_L = -60$
I_{Na}	$g_Na m_\infty(v)^3 h(v - E_{Na})$	$m_\infty(v) = 1/[1 + \exp(-\frac{v+30}{15})]$	$h_\infty(v) = 1/[1 + \exp(\frac{v+39}{3.1})]$ $\tau_h(v) = 1 + 500/[1 + \exp(-\frac{v+57}{-3})]$	$g_{Na} = 37$ $E_{Na} = 55$
I_K	$g_K n^4(v - E_K)$	$n_\infty(v) = 1/[1 + \exp(-\frac{v+32}{8})]$ $\tau_n(v) = 1 + 100/[1 + \exp(-\frac{v+80}{-26})]$		$g_K = 45$ $E_K = -80$
I_T	$g_T a_\infty(v)^3 b_\infty(r)^2 r(v - E_T)$	$a_\infty(v) = 1/[1 + \exp(-\frac{v+63}{7.8})]$ $b_\infty(r) = 1/[1 + \exp(-\frac{r-0.4}{0.1})]$ $- [1/[1 + \exp(4)]]$	$r_\infty(v) = 1/[1 + \exp(\frac{v+67}{2})]$ $\tau_r(v) = 7.1 + 17.5/[1 + \exp(-\frac{v+68}{-2.2})]$	$g_T = 0.5$ $E_T = 0$
I_{Ca}	$g_{Ca} c^2(v - E_{Ca})$	$c_\infty(v) = 1/[1 + \exp(-\frac{v+20}{8})]$ $\tau_c(v) = 1 + 10/[1 + \exp(\frac{v+80}{26})]$		$g_{Ca} = 2$ $E_{Ca} = 140$
I_{ahp}	$g_{ahp}(v - E_{ahp}) \left(\frac{CA}{CA+15} \right)$			$g_{ahp} = 20$ $E_{ahp} = -80$

[1]

Globus Pallidus

GPi and GPe were modeled similarly.

$$\begin{aligned}
 C_m v' &= -I_L - I_{Na} - I_K - I_T - I_{Ca} - I_{ahp} - I_{STN \rightarrow GP} \\
 &\quad + I_{GPe \rightarrow GPe/GPi} + I_{app} + I_{dbs} \\
 h' &= 0.75[h_\infty(v) - h]/\tau_h(v) \\
 n' &= 0.75[n_\infty(v) - n]/\tau_n(v) \\
 r' &= 0.2[r_\infty(v) - r]/30 \\
 CA' &= 1 \times 10^{-4}(-I_{Ca} - I_T - 15 \times CA)
 \end{aligned}$$

[1]

Where $I_{STN \rightarrow GP}$ is the synaptic current from the STN to the GPi & GPe, and $I_{GPe \rightarrow GPe/GPi}$ is the synaptic current from the GPe to the GPe or GPi.

Table 3 GP cell model equations and parameters

Current	Equation	Gating variables	Gating variables	Parameters
I_L	$g_L(v - E_L)$			$g_L = 0.1$ $E_L = -65$
I_{Na}	$g_{Na} m_\infty(v)^3 h(v - E_{Na})$	$m_\infty(v) = 1/[1 + \exp(-\frac{v+37}{10})]$	$h_\infty(v) = 1/[1 + \exp(\frac{v+58}{12})]$ $\tau_h(v) = 0.05 + 0.27/[1 + \exp(-\frac{v+40}{-12})]$	$g_{Na} = 120$ $E_{Na} = 55$
I_K	$g_K n^4(v - E_K)$	$n_\infty(v) = 1/[1 + \exp(-\frac{v+50}{14})]$ $\tau_n(v) = 0.05 + 0.27/[1 + \exp(-\frac{v+40}{-12})]$		$g_K = 30$ $E_K = -80$
I_T	$g_T a_\infty(v)^3 r(v - E_T)$	$a_\infty(v) = 1/[1 + \exp(-\frac{v+57}{2})]$	$r_\infty(v) = 1/[1 + \exp(\frac{v+70}{2})]$	$g_T = 0.5$ $E_T = 0$
I_{Ca}	$g_{Ca} s_\infty(v)^3(v - E_{Ca})$	$s_\infty(v) = 1/[1 + \exp(-\frac{v+35}{2})]$		$g_{Ca} = 0.15$ $E_{Ca} = 120$
I_{ahp}	$g_{ahp}(v - E_{ahp}) \left(\frac{CA}{CA+10} \right)$			$g_{ahp} = 10$ $E_{ahp} = -80$

[1]

Bias Currents

Bias currents for the healthy brain were simulated to maintain baseline firing rates of 70 Hz for the GPe, 80 Hz for the GPi, and 10 Hz for the STN. In the parkinsonian brain, we expect to see

an increase in bursting behavior and synchronization of the GPe and GPi neurons. Recent results (Hahn and McIntyre 2010) suggest that firing patterns in PD result from changes in the inputs of the basal ganglia. To achieve such results mathematically, the constant bias currents I_{app} were decreased. As such, the following bias currents were used to differentiate the healthy and parkinsonian brain.

Conditions	I_{app} for STN	I_{app} for GPe	I_{app} for GPi	
Healthy	33 uA/cm ²	20 uA/cm ²	21 uA/cm ²	
Parkinsonian	23 uA/cm ²	7 uA/cm ²	15 uA/cm ²	[1]

Sensorimotor Cortex

The current from the sensorimotor cortex to the thalamus is modeled as a 5 ms 3.5 uA/cm² monophasic current pulse with instantaneous frequencies drawn from a gamma distribution with an average rate of 14 Hz and a coefficient of variation of 0.2.

Deep Brain Stimulation

The deep brain stimulation current in the STN or GPi was modeled by adding the I_{dbs} term to the corresponding Hodgkin-Huxley type membrane potential differential equation. The three regimes of DBS are square, white noise, and pink noise pulses. Pink noise (1/f noise) is a signal with a power spectral density (power per frequency interval) that is inversely proportional to the frequency. White noise, on the other hand, has a constant power spectral density [7].

The default square pulse was modeled as a monophasic, 300 uA/cm² current density, 130 Hz frequency, 0.3 ms width pulse. The white noise and pink noise pulses were modeled using the dsp.ColoredNoise function in matlab, with the number of samples equal to the number of time steps during the simulation. These functions created noisy signals (vectors) with mean zero, the number of samples equal to the number of time steps, and amplitude varying between 8 and -8. As such, the noise was incorporated by setting $I(t)_{dbs,noise} = I(t)_{dbs,square} + 10 * noise(t)$, where $I(t)_{dbs,square}$ is the default square dbs pulse, and $noise(t)$ is the noisy signal at time t.

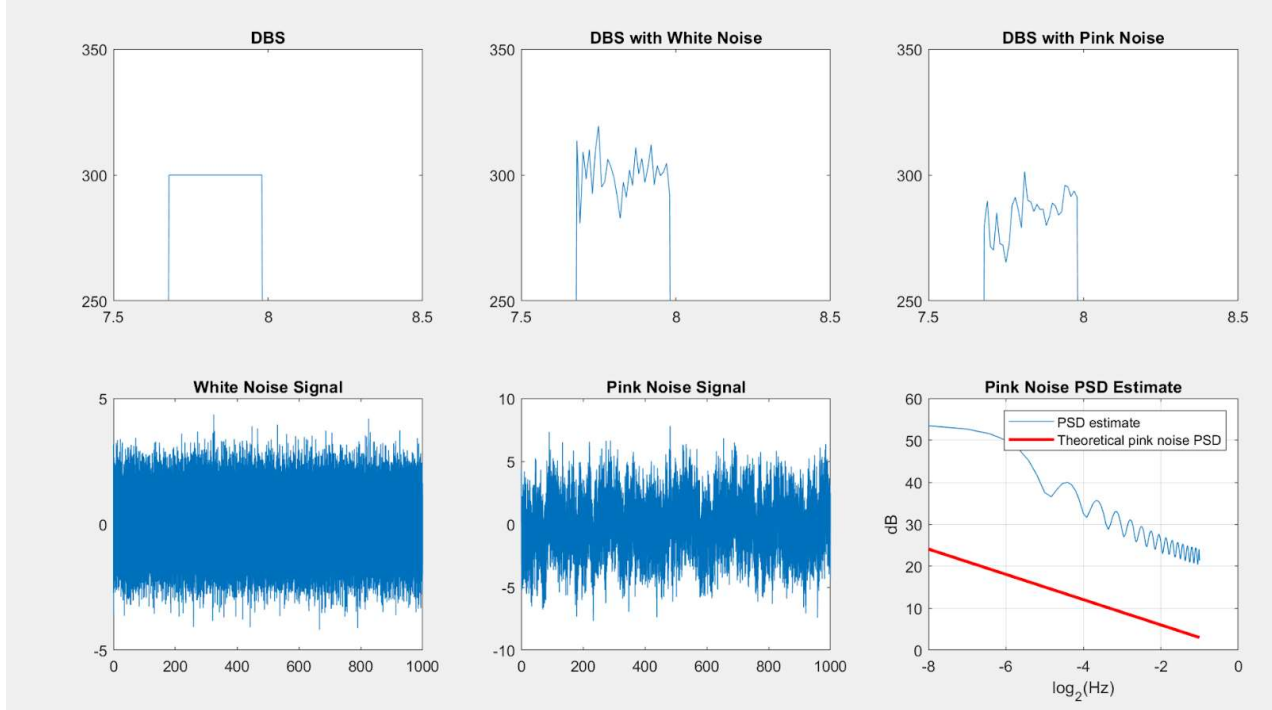


Figure 2: Stimulus regimes. **Top** Square pulse ($\mu\text{A}/\text{cm}^2$ vs. time [ms]), white noise pulse ($\mu\text{A}/\text{cm}^2$ vs. time [ms]), pink noise pulse ($\mu\text{A}/\text{cm}^2$ vs. time [ms]). **Bottom** white noise signal (unitless), pink noise signal (unitless), pink noise power spectral density of the DBS pulse (blue) as compared to theoretical pink noise power spectral density (red).

Synaptic Currents

Synaptic current from structure α to structure β is given by

$$I_{\alpha \rightarrow \beta} = g_{\alpha \rightarrow \beta} [v_{\alpha} - E_{\alpha \rightarrow \beta}] \sum_j s_{\alpha}^j \quad [1]$$

Where $g_{\alpha \rightarrow \beta}$ is the maximal synaptic conductance, and $E_{\alpha \rightarrow \beta}$ is the synaptic reversal potential. This sums over the presynaptic cells. Each synaptic variable s_{α}^j is given by the following differential equation

$$s'_{\alpha} = A_{\alpha} [1 - s_{\alpha}] H_{\infty}(v_{\alpha} - \theta_{\alpha}) - B_{\alpha} s_{\alpha} \quad [1]$$

where H_{∞} is the smooth approximation of the heaviside step function, and A_{α} and B_{α} control the synaptic time courses. For $\alpha = \text{GPi}, \text{GPe}, \text{STN}$, we take $A_{\alpha}, B_{\alpha}, \theta_{\alpha} = (2, 0.08, 20), (2, .04, 20), (5, 1, 30)$. The synapse parameters are given as

Synapses	Parameters
$I_{STN \rightarrow GPe}$	$g_{syn}=0.15, E_{syn}=0$
$I_{STN \rightarrow GPi}$	$g_{syn}=0.15, E_{syn}=0$
$I_{GPe \rightarrow STN}$	$g_{syn}=0.5, E_{syn}=-85$
$I_{GPe \rightarrow GPe}$	$g_{syn}=0.5, E_{syn}=-85$
$I_{GPe \rightarrow GPi}$	$g_{syn}=0.5, E_{syn}=-85$
$I_{GPi \rightarrow TH}$	$g_{syn}=0.17, E_{syn}=-85$

[1]

Solving Differential Equations

For each differential equation, we simply used the forward Euler method with timestep $dt=0.01$ sec. Each individual current from the differential equations above was calculated, and the voltage in each cell was updated.

Error Index

To determine the efficacy of deep brain stimulation on the parkinsonian brain, we used the same metric as [1] [6]. Because the thalamus is responsible for faithfully relaying signals from the sensorimotor cortex, the ratio of missed relays over total signals from the SMC gives a quantitative approximation of the efficacy of DBS.

Error Index = Missed relays in TH / total signals from SMC

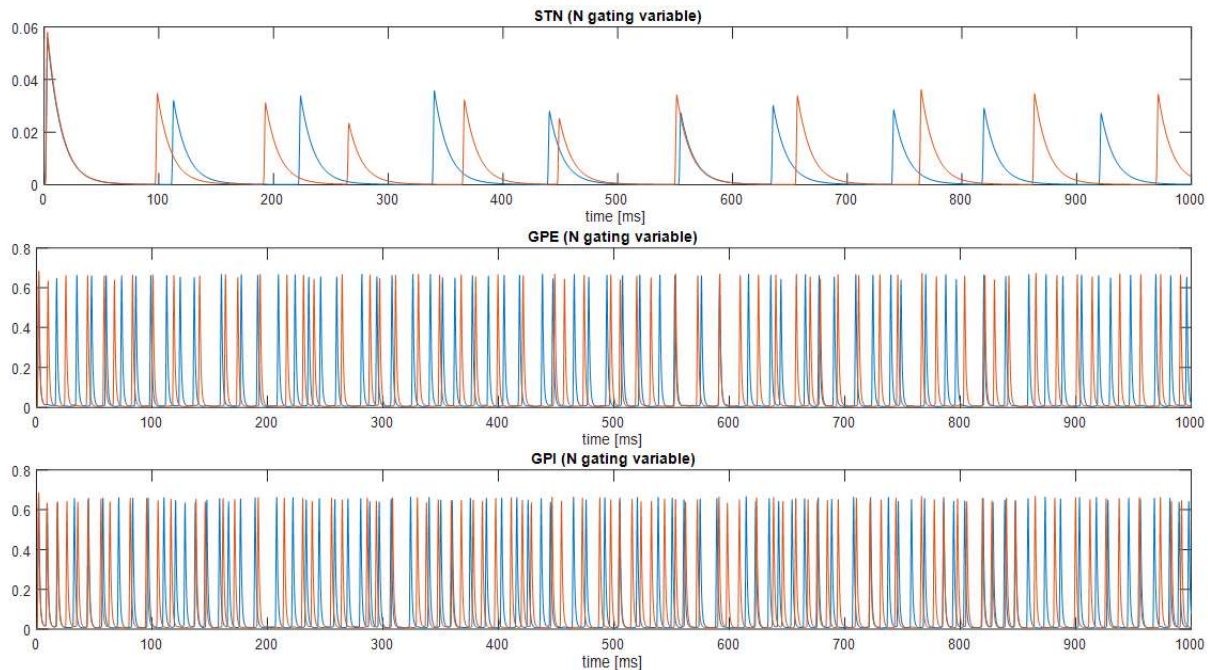
Stochastic Potassium Channels:

The Gillespie method is utilized to calculate the distribution of potassium channels in each discretized state [5]. There are 5 steps, representing the five possible configurations of the 4 potassium channel subunits (0 = fully closed, 1 = 1 subunit open, 2 = 2 subunits open, 3 = 3 subunits open, 4 = all subunits open). The transitions between each of these states are calculated using the individual channel forward and reverse rates. These can be calculated using the existing time constant and steady state channel functions in the So model and are voltage dependent. Each transition rate is weighted by the number of subunits in its corresponding direction. For example, for transitioning from the state of “fully closed” to “1 subunit open”, the forward channel opening rate is weighted by a factor of 4, as the fully closed state has 4 closed subunits. This is further weighted by the number of channels in that particular state. Similarly the closing rate is weighted by 0, as there are no available subunits to move to the closed state. This same logic is used for the other potential configurations. Lastly, The Gillespie method uses an exponential distribution to model the dwell time of the channels in a particular state. The total rate constant is defined as the sum of each of the individual rate constants, which is defined by the transitions between each potential state. For example, in our case, it is the sum of each of the weighted rates calculated above. Following our stochastic methodology, a random number is

calculated and the natural log of this number divided by the total transition rate defines the next “update time” where the channel configurations change. This follows from a simple isolation of “ τ ” from the exponential distribution formula. Therefore, for a larger number of channels, the simulation will take longer as there will be more necessary updates. Then a second random number is generated and normalized to our total transition rate previously defined. We then define a running sum of our transition rates. If this scaled random number is in a certain range, we update the channel state corresponding to that particular range. For a simple example of this entire process, let us suppose that we only have two rates corresponding to any abstract state 1 and 2, with $r_1 = 1$ and $r_2 = 2$. Our total transition rate would be $r_3 = 3$. Then, we simply generate our first random number, take the natural log, and divide by r_3 to get our random update time. Next, we define a second random number to define which of our states is changed. Let this random number be .5. We scale this to the total rate by multiplying $r_3 \cdot .5 = 1.5$. 1.5 is greater than r_1 but less than r_2 . Therefore, we update state 2 and perform some operation on the components in this state. In the context of potassium channels, we would add or subtract one channel from the current state. We repeat this process until we reach the predefined constant time step. Therefore, for a given time step, the channel states are continuously updated and finally returned to the forward Euler solver.

Section 3 - Results:

Channel Conductances of Each Model Formulation:



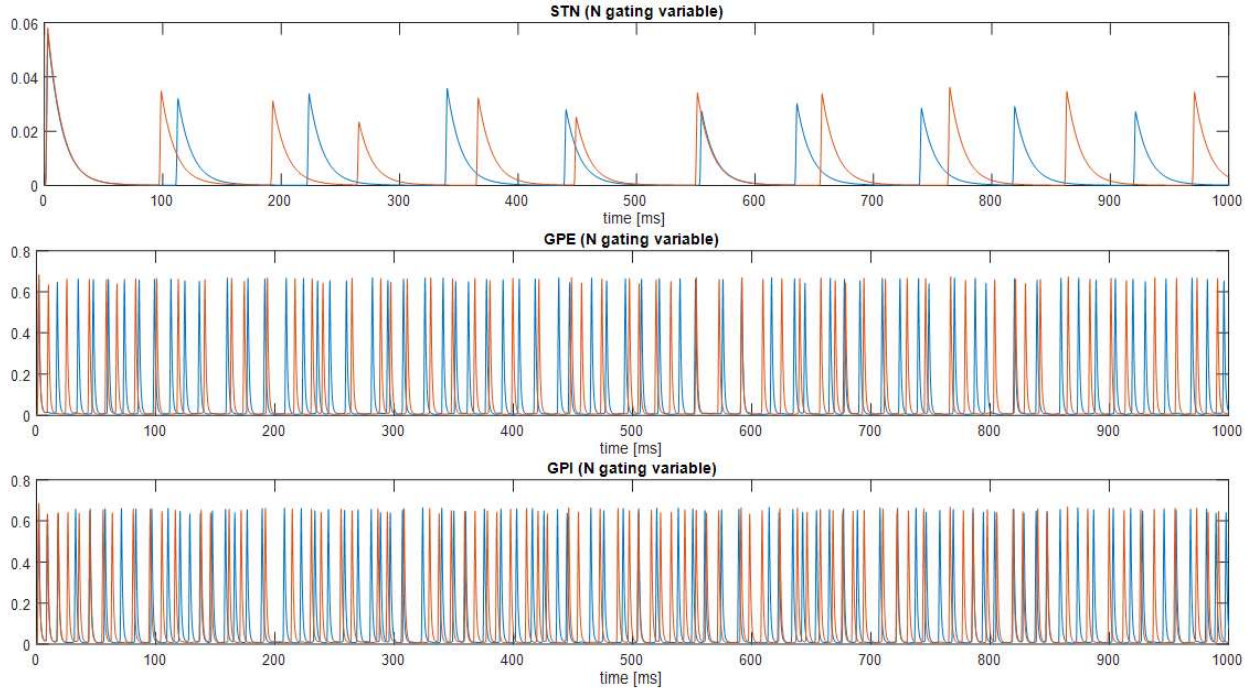


Figure 3: **Top** Maximal fractional conductance (fraction of the maximum conductance) of the stochastic potassium channels over time for each neuron subtype. **Bottom** Maximal fractional conductance (fraction of the maximum conductance) of the deterministic potassium channels over time for each neuron subtype.

Initially, we look at the gating variables to ensure that the values of our stochastic reformulated fractional maximal conductances accurately reflect the original deterministic version. Above, it is clear that this is the case. We can confirm that, in each of the three neuron subtypes, the fractional maximal conductance derived from the stochastic version of the HH equations has very similar amplitude to those from the original deterministic version. Additionally, the shape of each action potential matches up with their deterministic counterparts, as can be seen by the slowly recovering STN neuron action potentials and the more quickly changing GPI/GPE neuron action potentials.

Reproducing Results with Stochastic Channels:

Healthy condition:

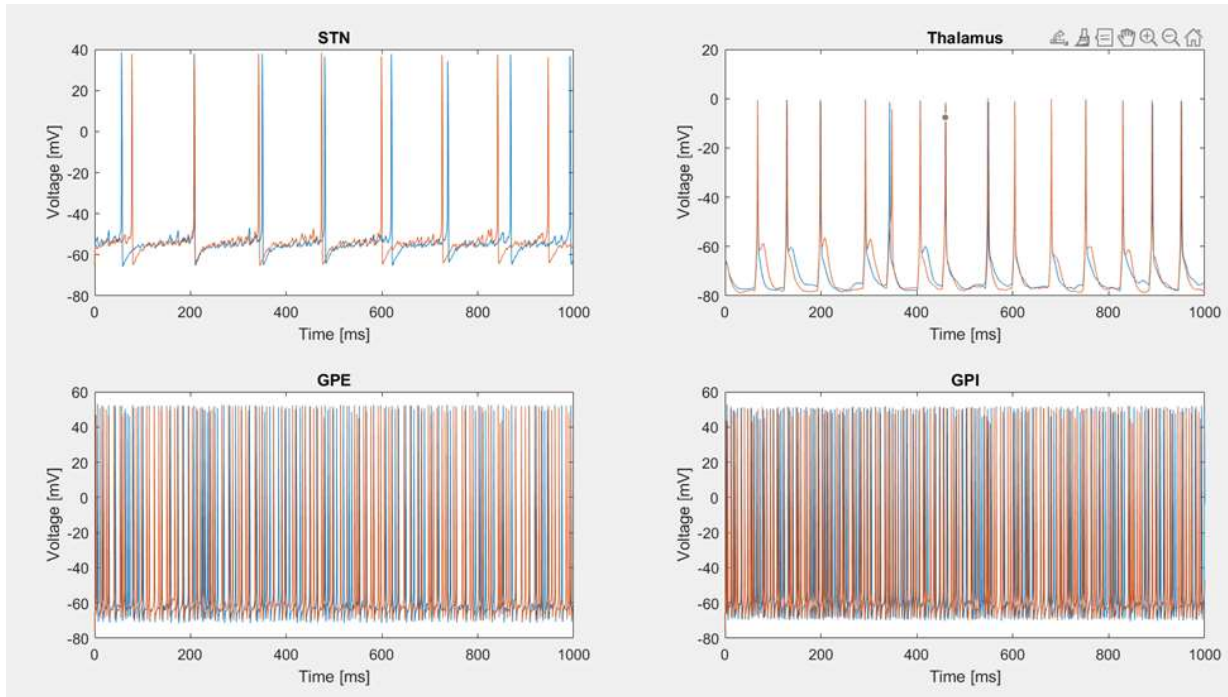


Figure 4a: Two neurons from each population within the basal ganglia under healthy conditions with stochastic potassium channels. Error index value of .05.

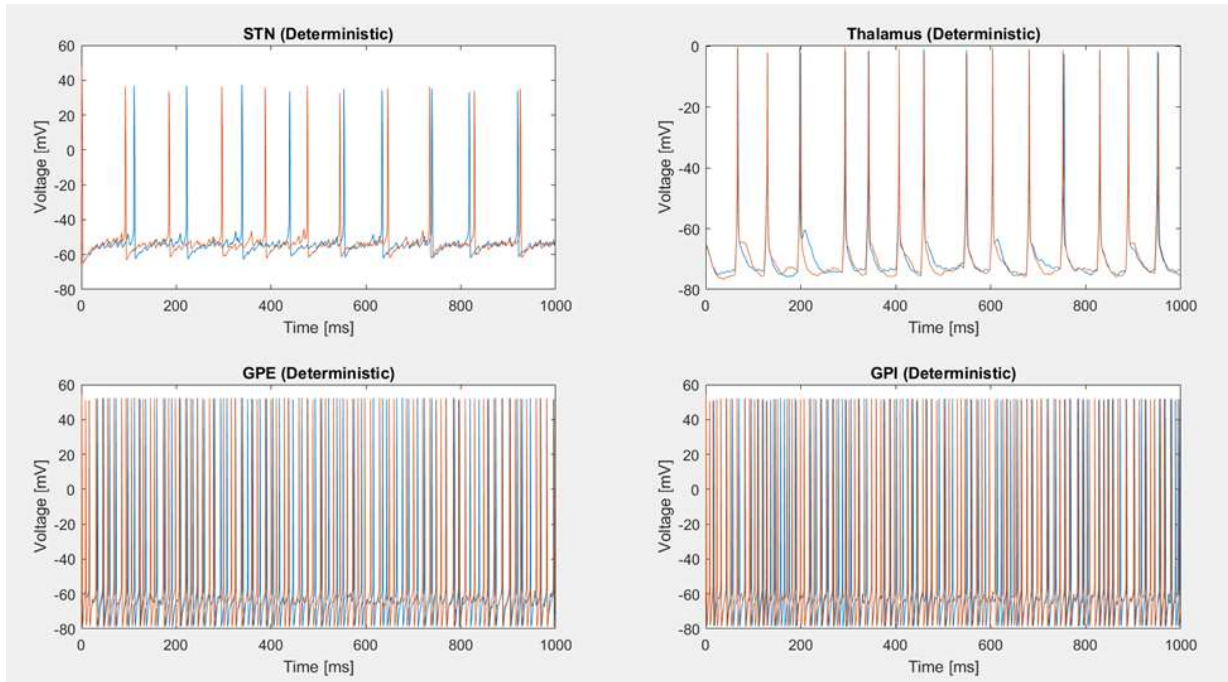


Figure 4b: Two neurons from each population within the basal ganglia under healthy conditions with deterministic HH equations. Error index value of .03.

Parkinsonian condition:

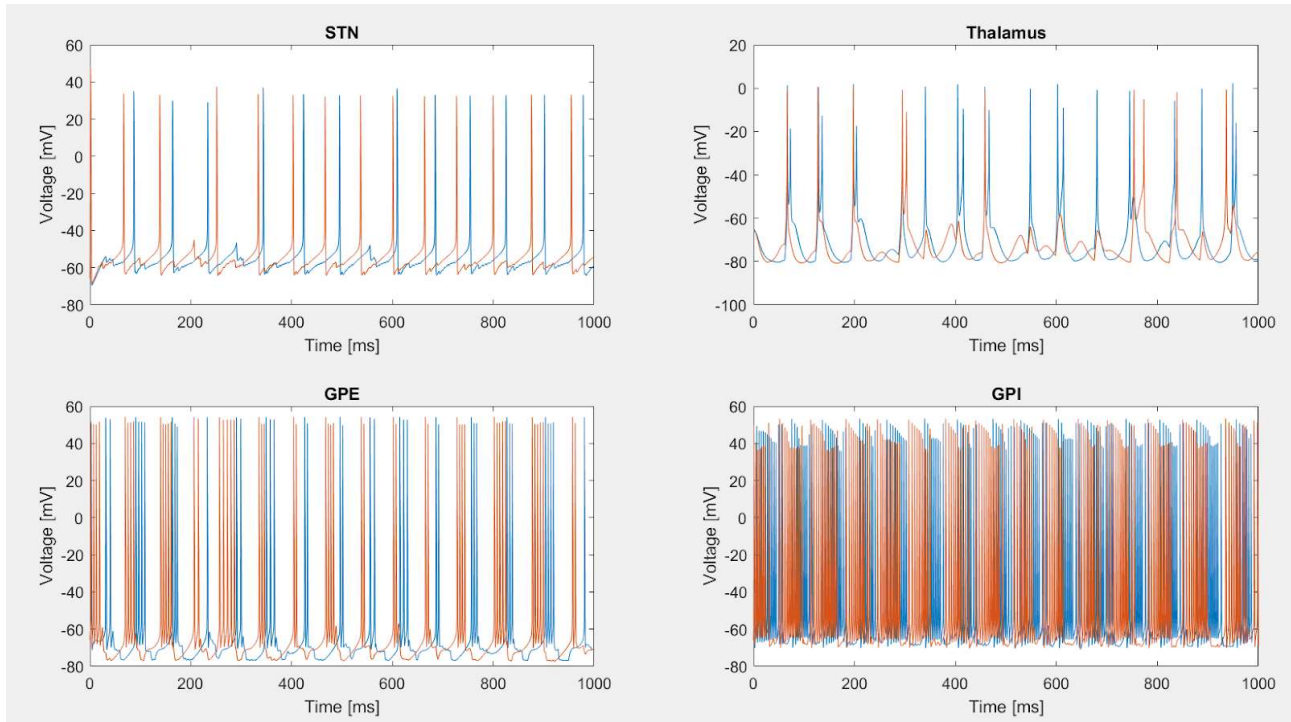


Figure 5a: Two neurons from each population within the basal ganglia under Parkinsonian conditions with stochastic potassium channels. Error index value of .71.

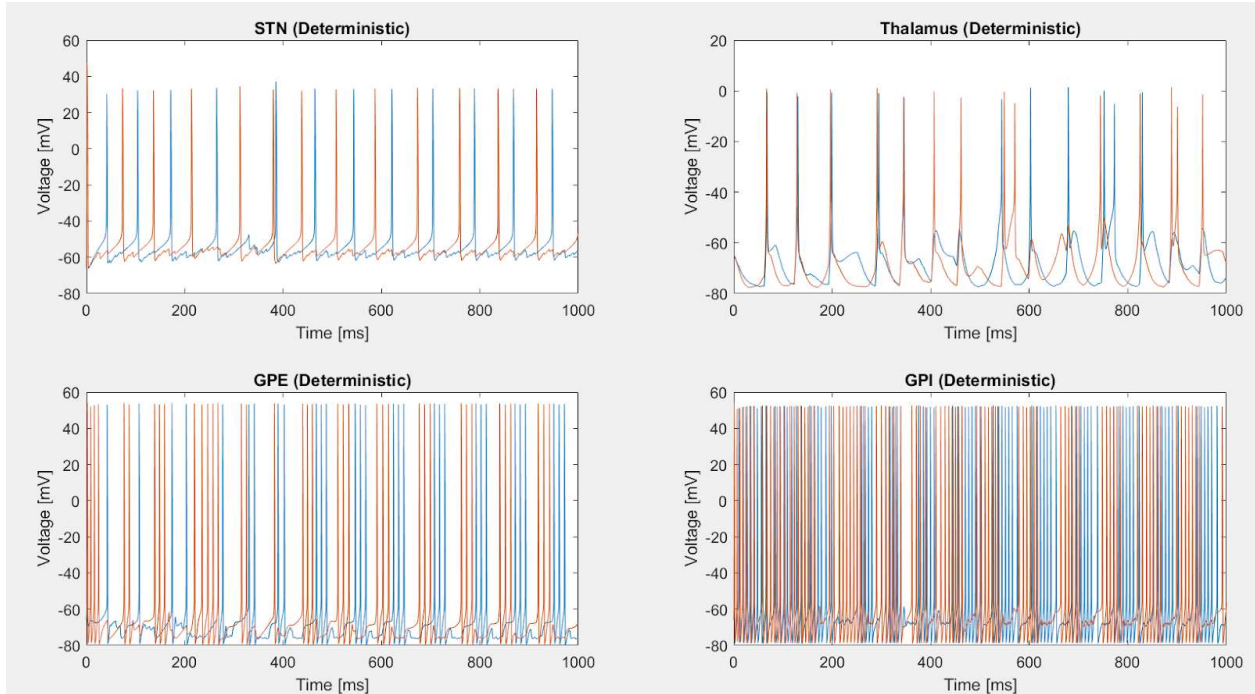


Figure 5b: Two neurons from each population within the basal ganglia under Parkinsonian conditions with deterministic HH equations. Error index value of .53.

As can be seen in Figures 4 and 5, at the network level, the underlying dynamics of the basal ganglia in healthy and Parkinsonian conditions are very similar across our two modelling approaches. In both the stochastic and the deterministic versions of the model, there is a general agreement for both Error Index values as well as the firing behavior of the important regulatory neurons (GPI/GPE). In the healthy condition, the error index value is low in both models, and the thalamus accurately relays signals from the sensorimotor cortex. Additionally, the GPE/GPI neuron activity is tonic and independent of one another. The neuron firing is uncorrelated, and seems to follow no set pattern. However in the Parkinsonian condition, the error index in both models rises to much higher levels (stochastic = .73, deterministic = .53), and the GPE/GPI firing becomes very rhythmic, with bursts of each individual neuron closely following the bursts of others in the cell population. This inhibitory firing pattern can be closely linked to “missed” spikes in the thalamic cell population, which explains the increased error index.

Parkinsonian condition with traditional DBS:

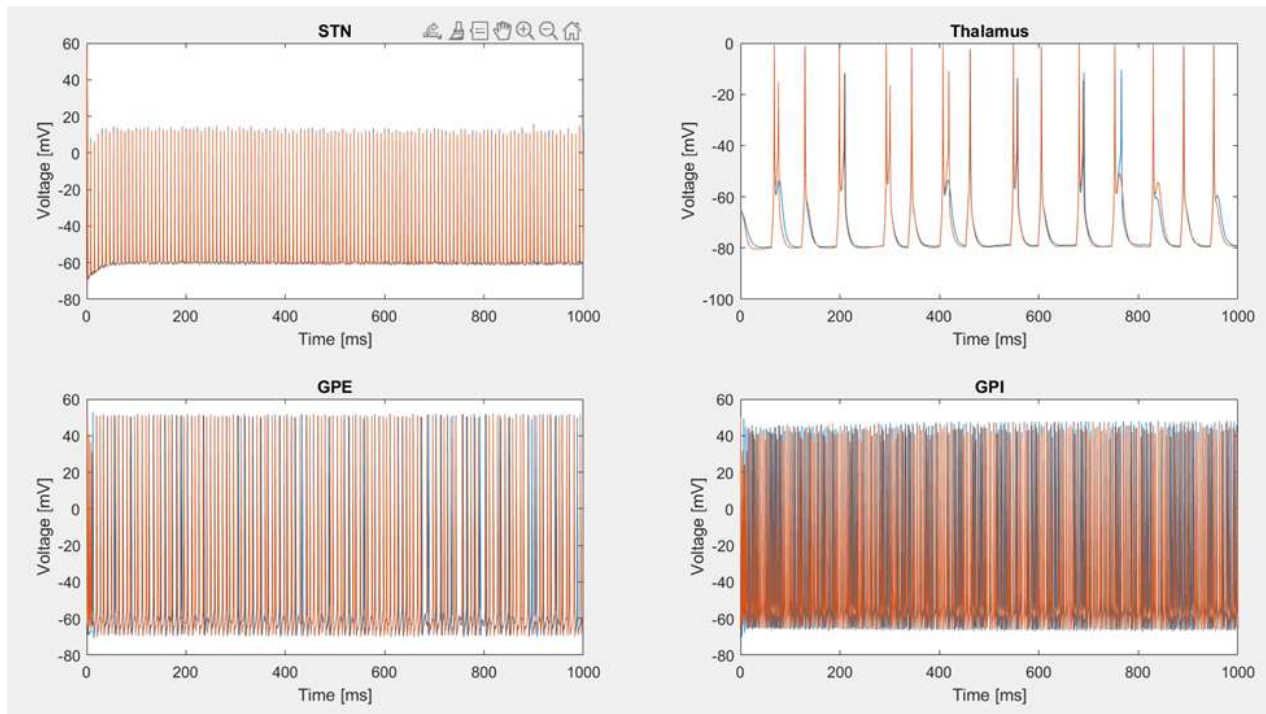


Figure 6a: Two neurons from each population within the basal ganglia under Parkinsonian conditions after high frequency stimulation (DBS) with stochastic potassium channels. Error index value of .28.

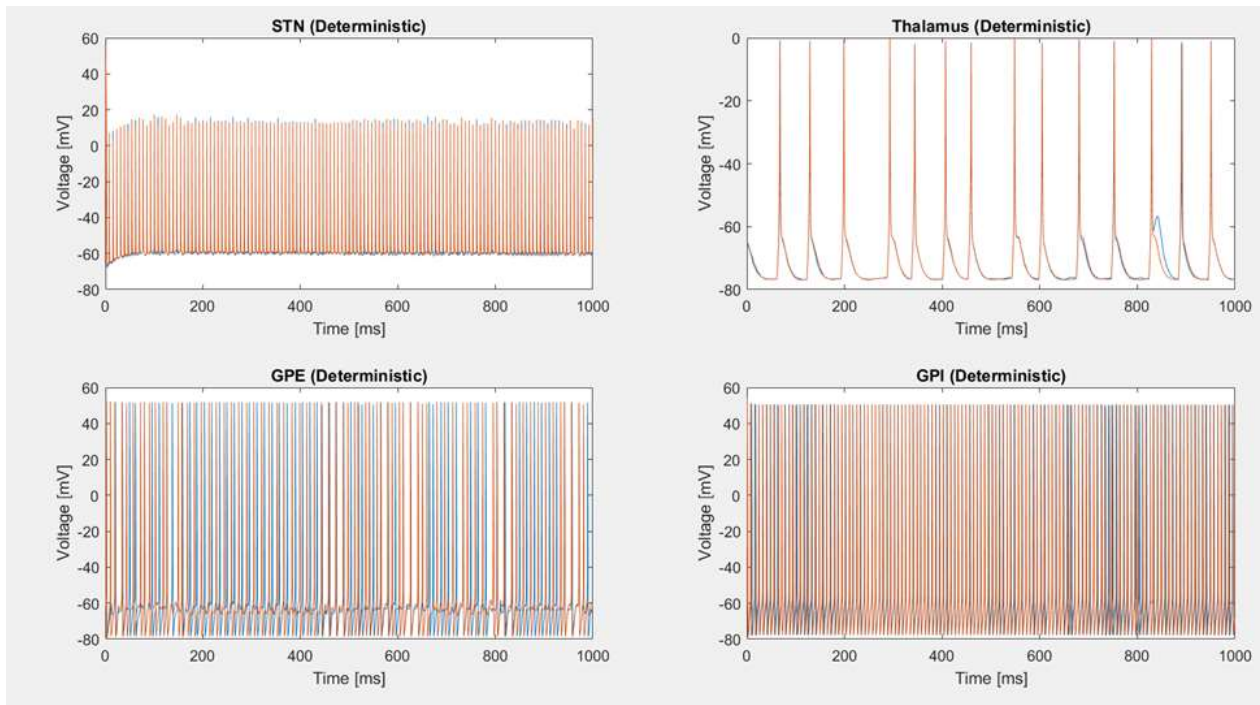


Figure 6b: Two neurons from each population within the basal ganglia under Parkinsonian conditions after high frequency stimulation (DBS) with deterministic HH equations. Error index value of .0.

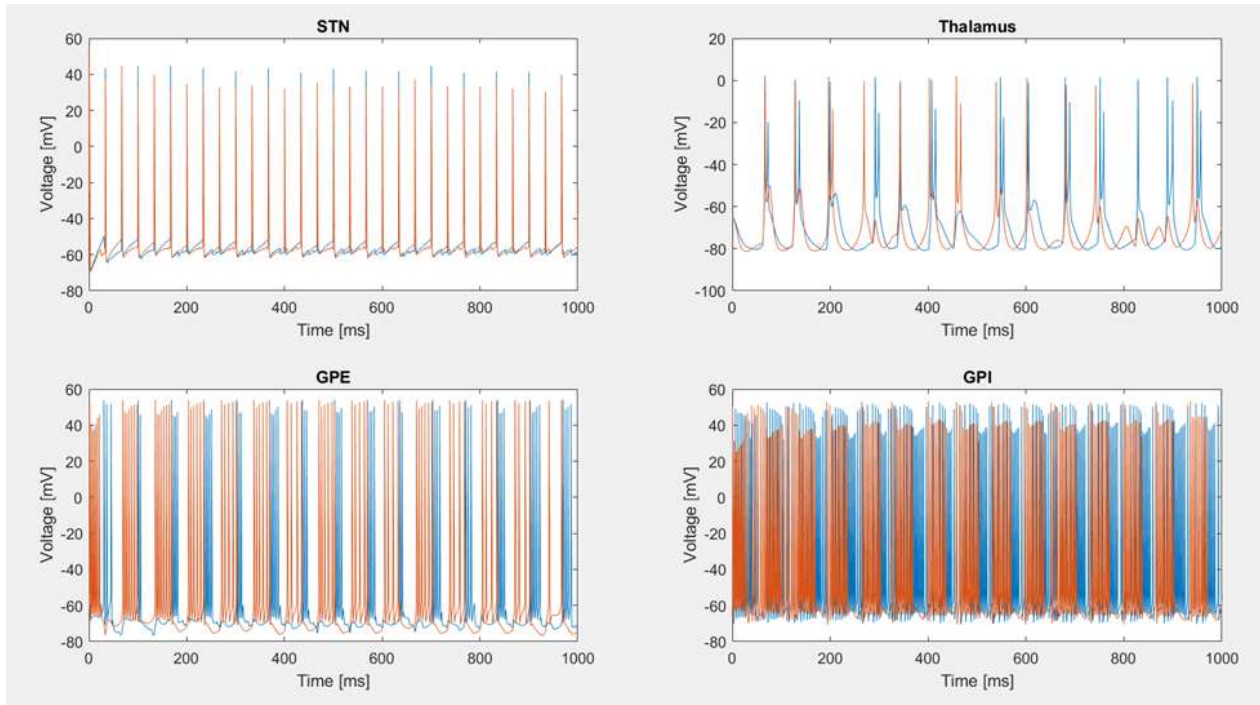


Figure 6c: Two neurons from each population within the basal ganglia under Parkinsonian

conditions after low frequency stimulation (DBS) with stochastic potassium channels. Error index value of .6.

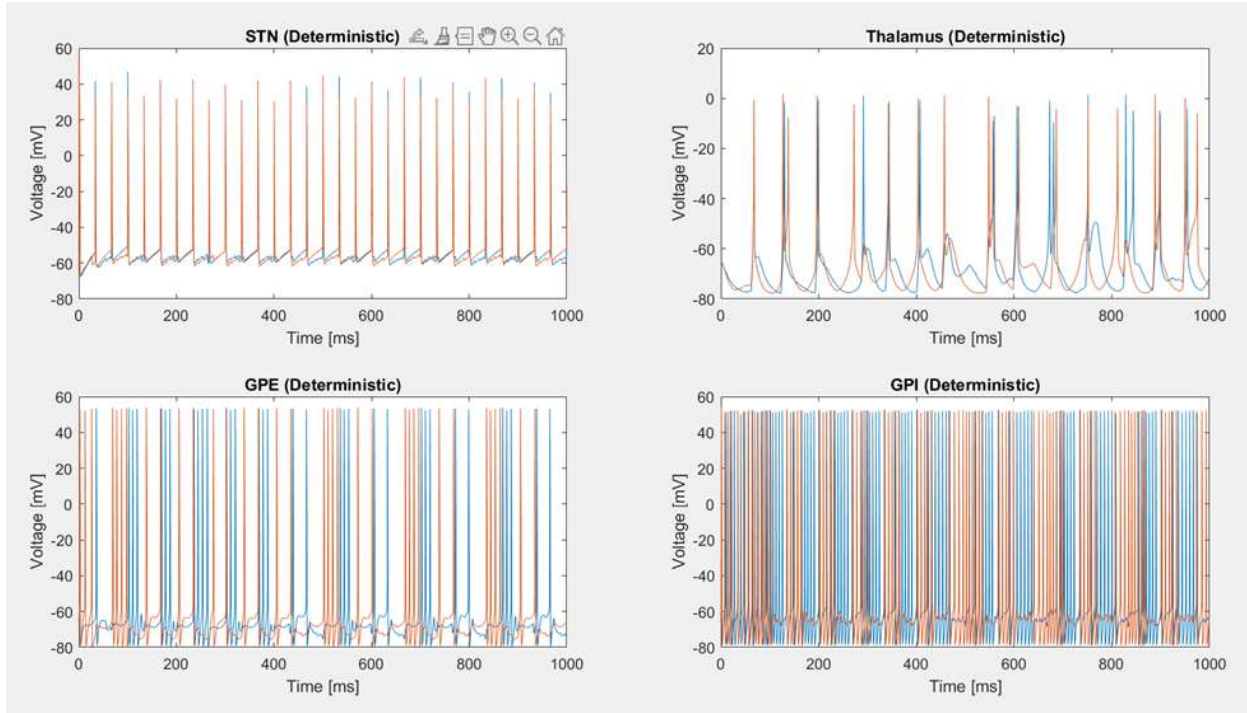


Figure 6d: Two neurons from each population within the basal ganglia under Parkinsonian conditions after low frequency stimulation (DBS) with deterministic HH equations. Error index value of .3.

DBS stimulus regimes have been determined to be most effective at high frequencies, with stimulation at lower frequencies (<50 Hz) often shown to be ineffective at best, and harmful at worst. Therefore, we show two different stimulus patterns, one at a higher frequency of 130 Hz, which has been demonstrated clinically effective, and a lower frequency of 30 Hz, which is ineffective. Our modelled results agree with both the deterministic model (Figure 6b,d) and clinically observed results. High frequency stimulation effectively decreases the error index (Stochastic model: from .71 to .28, deterministic model: from .53 to 0) and reduces the GPE/GPI firing aberrations. In contrast, low frequency stimulation seems to have very little or no effect (Stochastic model: from .71 to .6, deterministic model: from .53 to .3). Additionally, the GPE/GPI firing is still relatively rhythmic and synchronized within the population in the low frequency case, while in the high frequency case, the firing returns to the pattern demonstrated in the healthy condition.

Parkinsonian condition with noisy DBS:

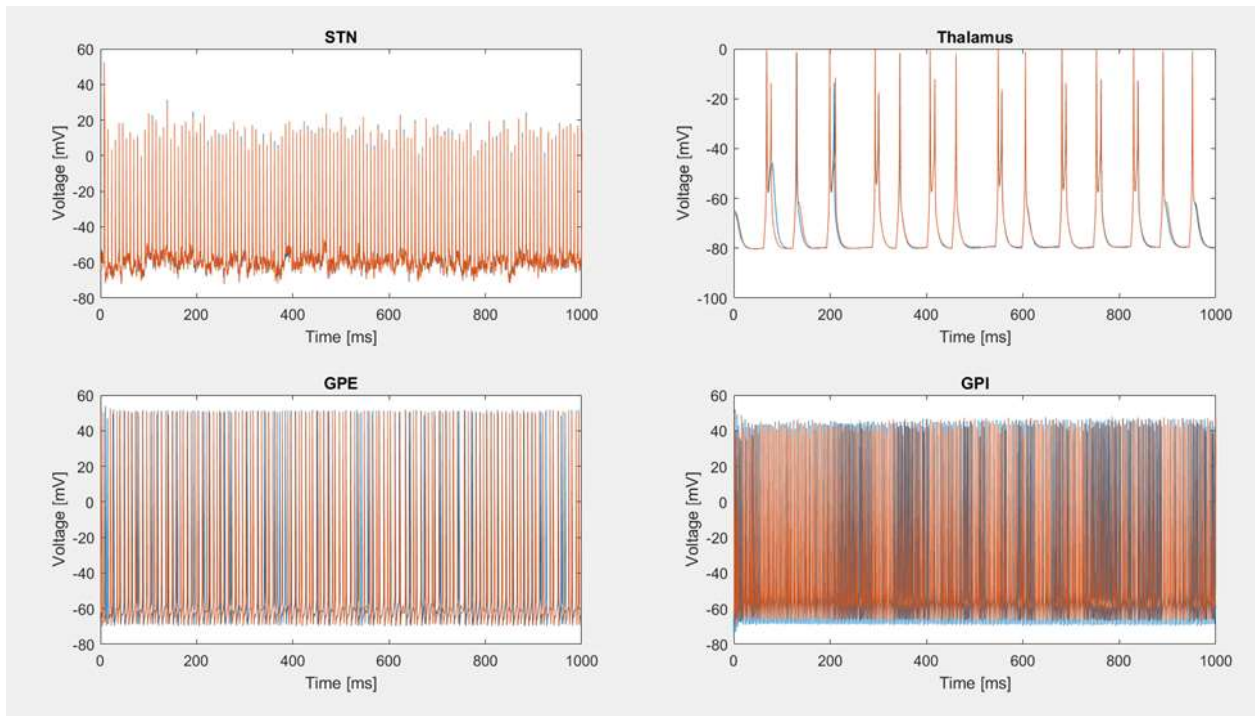


Figure 7a: Two neurons from each population within the basal ganglia under Parkinsonian conditions after pink noise stimulation with stochastic potassium channels. Error index value of .28.

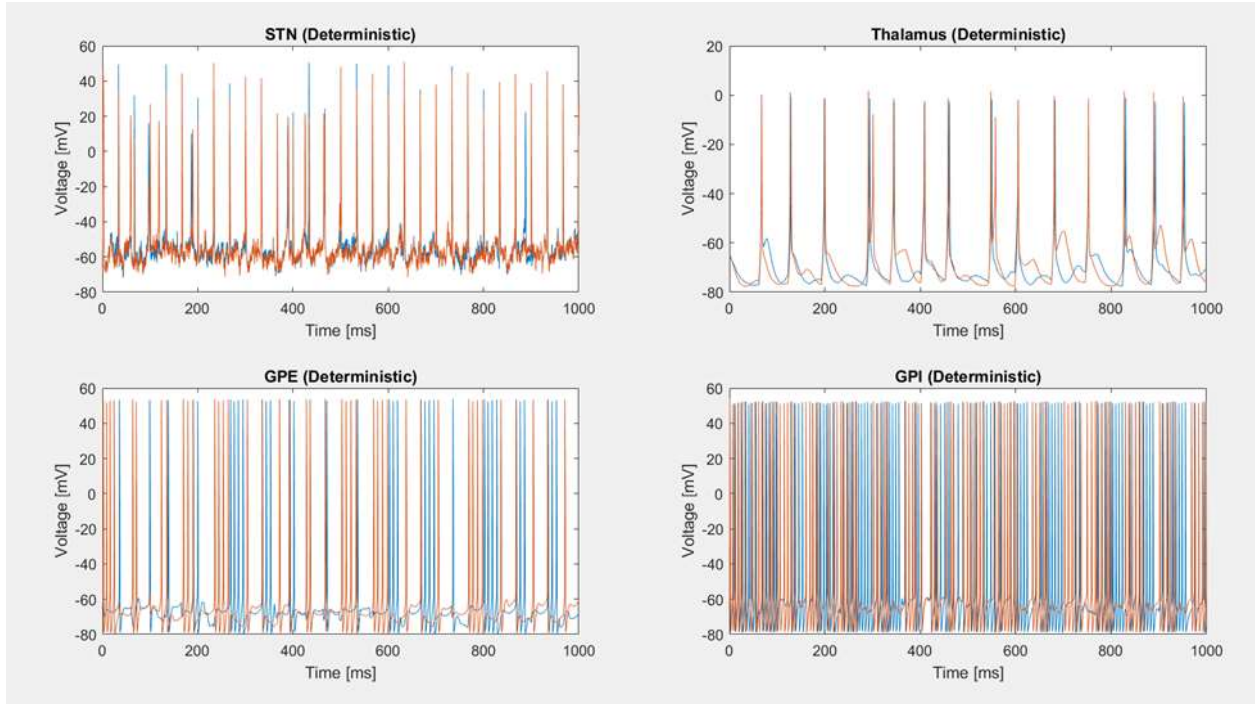
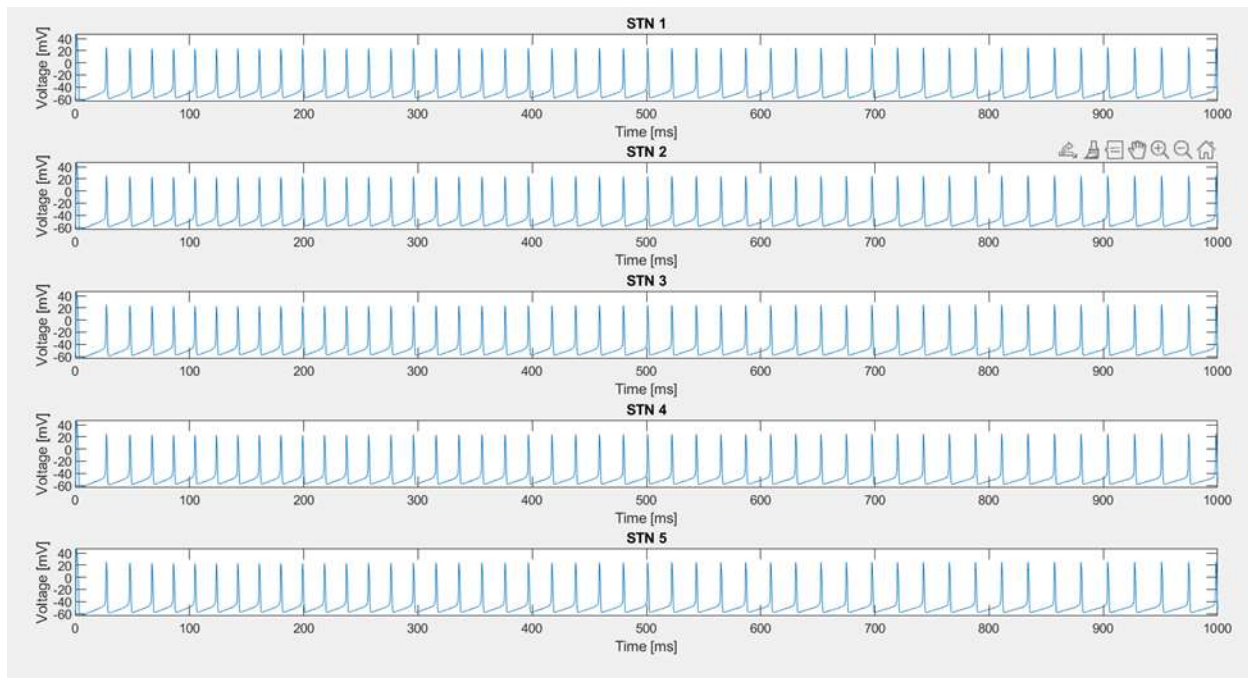


Figure 7b: Two neurons from each population within the basal ganglia under Parkinsonian

conditions after pink noise stimulation (DBS) with deterministic HH equations. Error index value of .19.

With a noisy high frequency stimulus (pink noise added throughout the original 130 Hz stimulus), similar efficacy is demonstrated to the original high frequency stimulus. The error index decreases from .71 to .37 in the stochastic model and from .53 to .23 in the deterministic model. GPE/GPI firing patterns more closely resemble the healthy condition in the stochastic model, while the deterministic model still includes bursting behavior. However, the firing of each neuron within the GPE/GPI population seems to be more uncoupled than the pure Parkinsonian condition, which resembles a transition to behavior more adjacent to the healthy condition.

Stimulus Entrainment:



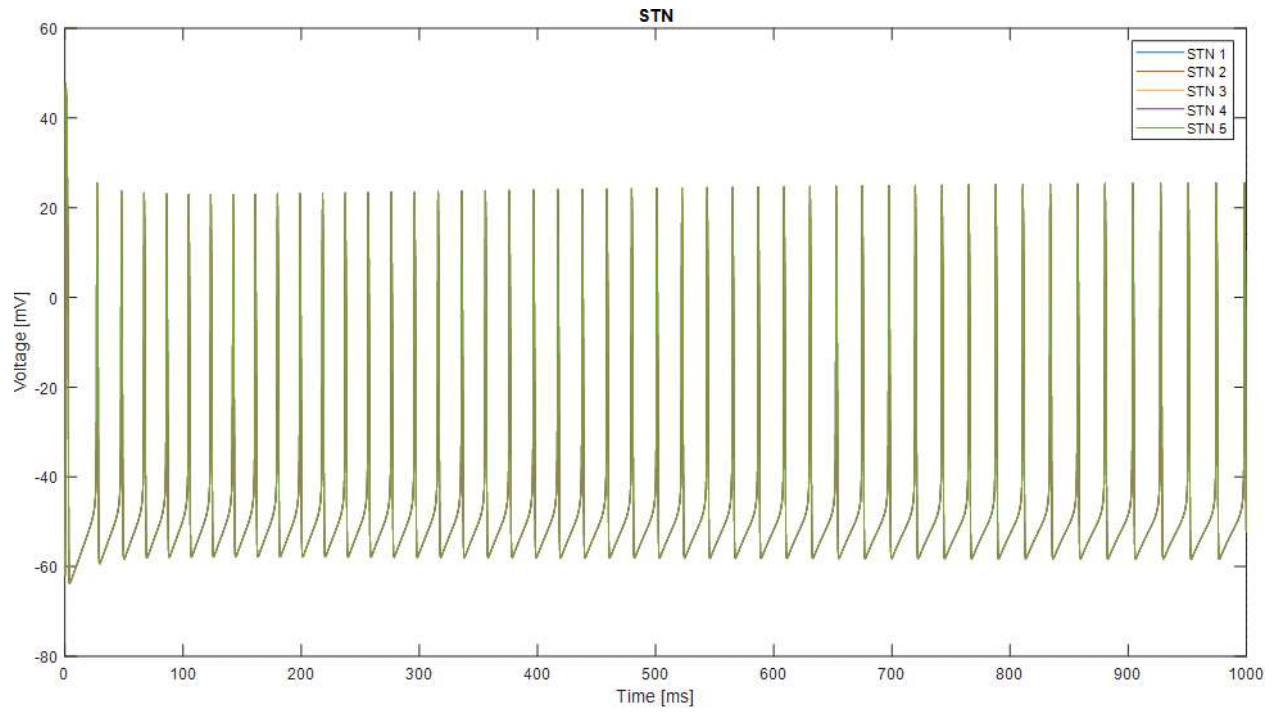


Figure 8: **Top** 5 isolated (no network connectivity) deterministic STN neurons with identical initial conditions receiving constant DC stimulus. Each fire at exactly the same time. **Bottom** Same 5 neurons' voltage traces superimposed.

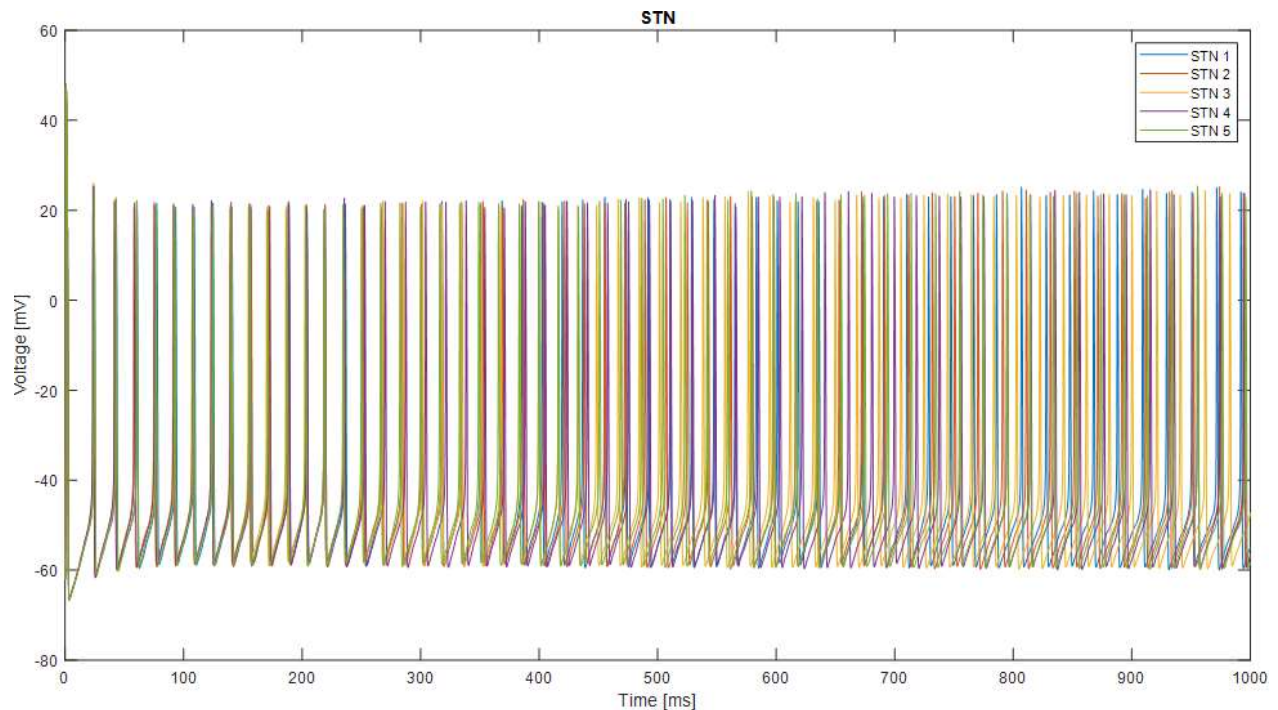


Figure 9: 5 isolated (no network connectivity) stochastic STN neurons with identical initial conditions receiving constant DC stimulus. Each fire synchronously at stimulus onset ($t = 0$ ms), and slowly desynchronize randomly.

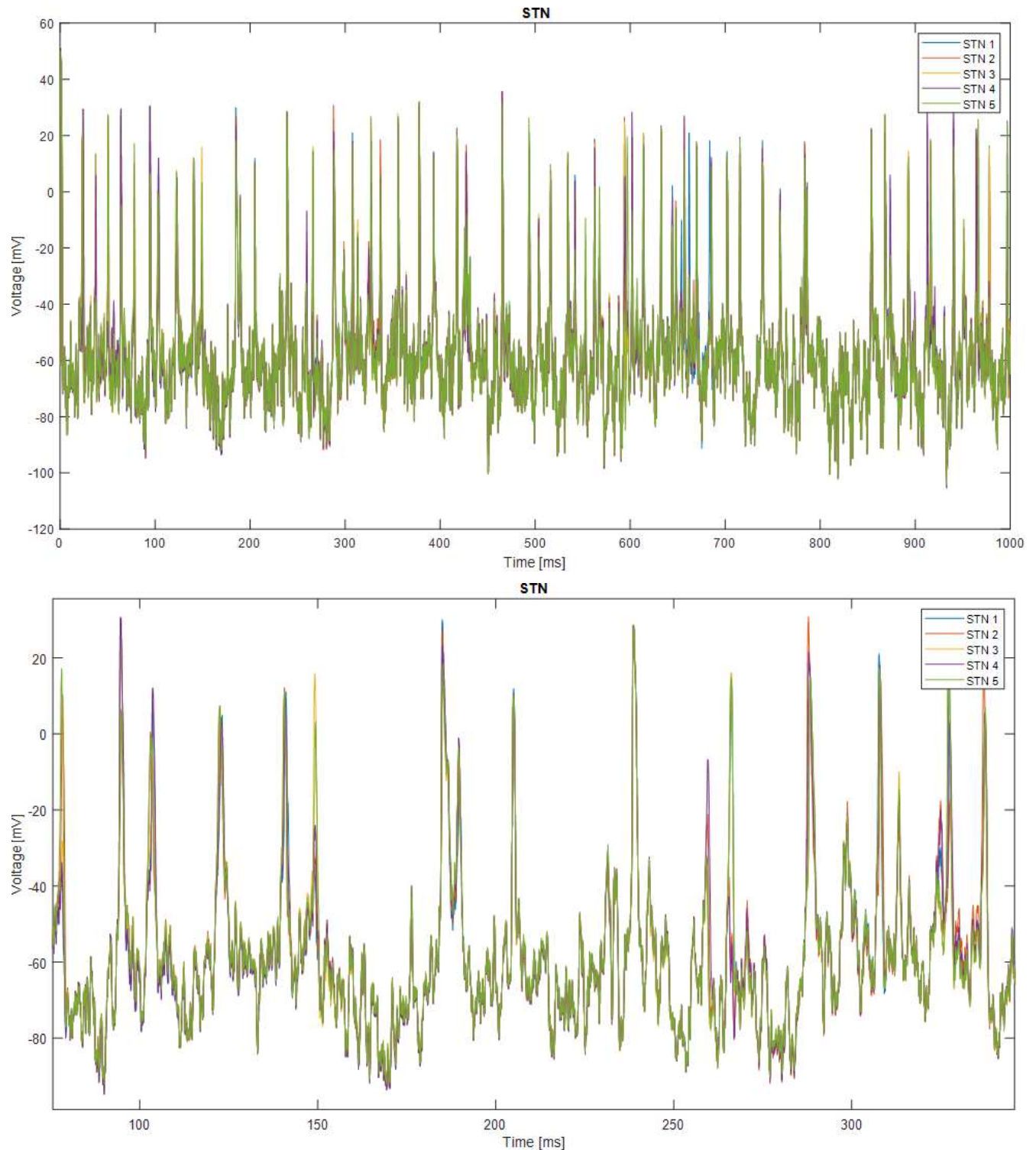


Figure 10: **Top** 5 isolated (no network connectivity) stochastic STN neurons with identical initial conditions receiving pink noise stimulus. Each fire at exactly the same time. **Bottom** Zoomed in version of the Top panel, showing more clearly that the spikes in each neuron are synchronized.

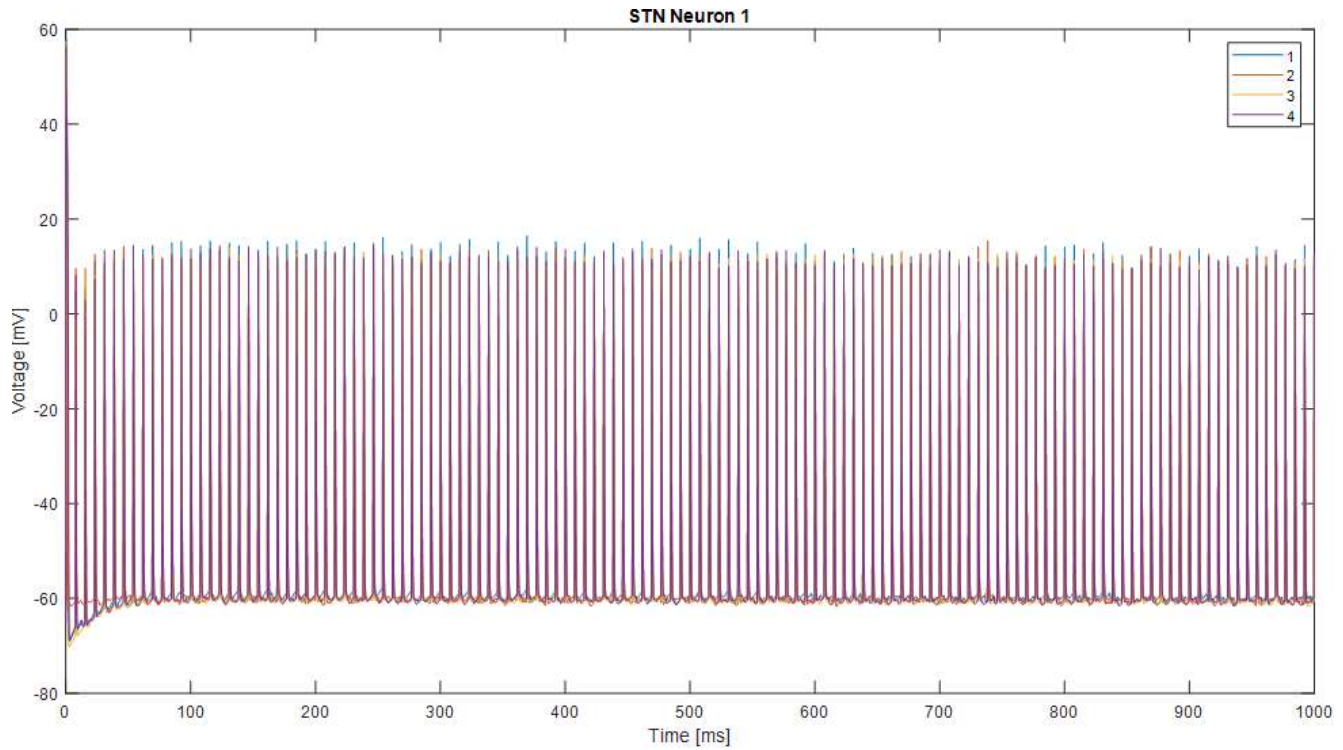


Figure 11: 5 STN neurons in basal ganglia network under DBS pink noise stimulus. Spiking is synchronized at all points in time.

To investigate the phenomenon described by Mainen et. al. in our own model system, we isolated STN neurons, removing them from the overall network in both the stochastic and deterministic models. After applying a constant DC input to both of these isolated neurons, we found that the model system accurately replicated the previous results. In particular, over time, the deterministic model demonstrates no fluctuations, firing with perfect reliability and synchrony in each trial (Fig. 8). In contrast, with the stochastic model, while the frequency of firing remained constant, the exact timing of the action potentials varied from trial to trial, and gradually after the stimulus onset, the different trials experienced a random, gradual desynchronization (Fig. 9). In contrast, when a noisy input was applied to the stochastic model, each trial had voltage traces that matched up almost exactly, indicating a much higher spike reliability (Fig. 10). However, when realistic DBS current magnitudes were applied the spikes began matching up much more closely (Fig. 11).

Discussion of Results and Physiologic Implications:

For the sake of brevity, the main point of the discussion will focus on Fig. 11. In all other results, the results of the stochastic model are relatively accurate. While there may be small discrepancies and improvements imparted by each model formulation, the implications for DBS are much more interesting. Fig. 9 and 10 both demonstrate the phenomenon described by Mainen et. al. is accurately replicated in the stochastic model? The question becomes, why is this not

present in the network level simulation? The first answer to this question resides in the literature. Even now, it is not clear what the implications of this increased spike reliability is at the network level. While previous works are relatively confident in describing the single neuron response characteristics and potential mechanisms, network fluctuations have not been extensively studied. This makes sense as well. If we stimulate a small subset of cells with a constant DC input, and the overall firing rate remains the same, even with different spike timings, it does not seem likely that this will have a very large effect on the behavior of an entire network of neurons. However, that is not to say that this effect is not important. It is hypothesized that the reason that neurons respond with greater reliability to noisy inputs is because noisy inputs are more natural. Imagine any neuron; that neuron is subject to a variety of excitatory and inhibitory presynaptic inputs. These inputs will all fire at different times, and when we look at the overall signal over time, it is very likely to look exactly like a Gaussian white or pink noise process. Now what does this mean for the network? Because spike reliability is lower for constant DC inputs, the exact timing of each individual cell is inconsistent. If we increase the scale of this inconsistency to multiple neurons in the network and these neurons synapse onto the same postsynaptic neuron, it is very likely that the postsynaptic neuron will receive a noisy signal that is not at all similar over multiple trials. Therefore, we could expect that an experiment recording the behavior of this single neuron would be inconsistent, depending on the scale of the unreliable firing. However, in our model, we do not consider this possibility, and the number of neurons with inconsistent firing may not be adequate to evoke this possibility. A second answer to this question lies in the current magnitude of traditional DBS, and whether this effect would ever be realized. In traditional DBS, the current magnitude is much larger than the current magnitude that evoked the behavior in Figures 9-11. Therefore, in our simulations of DBS, the effect of noise may be overridden by the large current magnitude. However, this does not mean that it is impossible for the mechanisms described by Mainen et. al. to play a role in therapeutic consequences of DBS. Note that DBS stimulation is spatially variant, with the voltage imposed by the stimulation falling off at greater distances from the electrode. Potentially, this means that certain tissue receives input that may cause fluctuating responses. However, our model is not fit to capture this either, as all STN neurons have the same high magnitude input.

Section 4 - Summary and Conclusion:

In this work, we show that a stochastic reformulation of the original deterministic basal ganglia model for Parkinson's, recapitulates much of the basic behavior and metrics of Parkinson's disease of the original model. Namely, we find that GPE/GPI firing and the error index metrics are retained from the original model. Although there are some small differences in therapeutic efficacy and baseline scores when switching between the two model formulations, they still are in general agreement. Additionally, we find that our stochastic reformulation demonstrates a more realistic response to stimulus, including the variable fluctuations found by Mainen et. al. In

our model, single neuron recordings show that there is low reliability of neuron firing in response to a constant DC input, and the repeatability of each trial is similarly low. In contrast, in response to a noisy input, there is high reliability, and it is possible to accurately replicate the results from trial to trial. However, the implications of this are not clear for Parkinson's disease. It is entirely possible that the high current magnitude of DBS may override this effect. Additionally, when there is the added feedback of the various regulatory elements of the cortico-basal ganglia-thalamo-cortical loop network into the STN may diminish the effect of the noisy inputs. In essence, when integrating many more signals, there may be a loss of relative impact of our noisy stimulus. Therefore, in terms of implications for DBS, there is much more to be investigated.

Section 5 - Audience Responses:

Would it be possible to use a white noise or pink noise stimulus with DBS? Would power consumption allow for this?

This is an interesting question because it spans the translational implications. I would say that power is most likely not the most significant concern. The power fluctuations in pink and white noise signals are not always so large such that they are unrealizable. I think one issue is actually implementing the waveform, though. These signals have very quick fluctuations, and it might be difficult to accurately represent in a clinical setting. That combined with the power issue may make it more difficult to implement. However, with more investigation, it is not unrealistic to imagine this could be used as it is physically possible, although not as easy as traditional square waves.

Are stochastic ion channel behaviors in general more realistic than deterministic behaviors? Or are there reasons to use one vs. the other? It seems like the stochastic model is simply better as it mimics actual neuron response to different stimulus types. Why is this not always used in computational neuron models?

I think the answer to this lies in the computational time. Even with the Gillespie method, the simulations took at least 30 times as long as the deterministic versions of the same equations. When this is scaled to more than just potassium channels it is even more time consuming. In general, we believe that the stochastic gating is more realistic than the original HH gating variables. This can be seen in single channel recordings as well. If you look at the conductance of single channels, you will find that they switch on and off randomly over time. This is hypothesized to be due to random thermal noise. Therefore, the stochastic models replicate this behavior almost exactly. However, it seems in most applications that replicating this is not

essential. In fact, it was only used in our version because we wanted to see if there was any implication to the spike reliability phenomena in DBS.

Section 6 - References:

- [1] So, RQ., Kent, AR., Grill WM. Relative Contributions of local cell and passing fiber activation and silencing to changes in thalamic fidelity during deep brain stimulation and lesioning: a computational modeling study. *J Comput Neurosci.* 2012; 32(3), 499-519
- [2] Armstrong, MJ & Okun MS. Diagnosis and Treatment of Parkinson's Disease: A Review. *JAMA.* 2020; 323(6):548-560
- [3] Mainen, Z. & Sejnowski TJ. Reliability of Spike Timing in Neocortical Neurons. *Science.* 1995; 268(5216), 1503-1506
- [4] Gal, A & Marom, S. Entrainment of the intrinsic dynamics of single isolated neurons by natural-like input. *J Neurosci.* 2013; 33(18), 7912-7918
- [5] Kispersky, T. & Whilte, JA. Stochastic methods of ion channel gating. *Scholarpedia.* 2008 doi:10.4249/scholarpedia.1327
- [6] Rubin, JE. & Terman, D. High frequency stimulation of the subthalamic nucleus eliminates pathological thalamic rhythmicity in a computational model. *Journal. Comput Neurosci.* 2004, 16(3), 211-235
- [7] Ward, LM., & Greenwood, PE, 1/f noise. *Scholarpedia.* 2007, doi:10.4249/scholarpedia.1537

Section 7 - Codes:

Used:

So Basal Ganglia Parkinson's model:

All components described extensively in the Methods above. In essence it is simply a large-scale version of the traditional HH neuron networks. Each of the individual cell populations are initialized for a certain number of cells and timesteps. These vectors store the voltage of the population over the simulation, which is done with the forward Euler method. The connectivities, currents, and cell parameters are described above in the methods. Note that this function calls

many functions for the gating variables and error index calculations. These functions must also be included. This forms the backbone of the additions we make.

Created:

Stochastic Potassium Markov Chain update function:

Uses Gillespie method described in Methods section to dynamically update the channel states of the potassium channel populations for each of the three neuron subtypes. Uses the forwards and backwards transition rates of the ion channels to calculate the transition probabilities. This function accepts four arguments: the current voltage, the current time, the desired time step, and the current state of the channel population. Using this, it will calculate how many updates to the channel population occur within the given time step using the current voltage. A lower time step results in higher resolution results, as the voltage is more accurate to the current time.

Stochastic model:

Replace all of the “N” gating variables in the original deterministic So model with the total number of completely open channels divided by the number of total channels multiplied by the original maximal conductance, g, of the channel. The total number of channels can be changed in the initial code block. The completely open channels are the channels at index 5 of the vector containing the channel states, and represent the channels with all subunits open. A small number of channels (<500) is usually insufficient, and will cause very noisy measurements. We use 15,000 which increases the time duration of the simulation and can be decreased. Even 1000 channels will show similar results. Lastly, we ensure that within the forward Euler method loop, we loop over every single neuron in our population and update its channel population.

Single STN neuron models:

First set all connectivity parameters in the original So model to 0 such that the input from other cells into the STN is terminated. Optional steps include also deleting all the other neuron subtypes so that their differential equations do not need to be updated. In the deterministic model this leads to very small time savings. In the stochastic model this can simply be replaced by commenting out the functions that update the channel population states for the unused GPE/GPI neurons. Lastly, initialize the STN neurons in the population to have identical initial conditions with a preset seed for the random number generator. Our function uses ‘twister’,1.

Noisy Signals:

To create the noisy signal, we simply define initial square waves similar to [1]. Then, we use MATLAB's built in "colored.noise" functions to generate identical length noisy signals centered on 0. We then simply add these two signals together. In the function, we define parameters such as pulse amplitude, noise amplitude, beta factor (for pink noise - how fast the power spectral density decreases). Lastly, we can plot power spectral density (to verify signal characteristics qualitatively).